Protein Expression and Purification 178 (2021) 105767

Contents lists available at ScienceDirect

Protein Expression and Purification

journal homepage: www.elsevier.com/locate/yprep

# Expression and functional identification of two homologous nicotine dehydrogenases, NicA2 and Nox, from *Pseudomonas* sp. JY-Q

Jun Li [a], Mingjie Shen [a], Zeyu Chen [a], Fanda Pan [b], Yang Yang [b,**], Ming Shu [b], Guoqing Chen [a], Yang Jiao [c], Fuming Zhang [d], Robert J. Linhardt [d], Weihong Zhong [a,*]

[a] College of Biotechnology and Bioengineering, Zhejiang University of Technology, Hangzhou, 310032, China
[b] Technology Center, China Tobacco Zhejiang Industrial Co., Ltd., Hangzhou, 310009, China
[c] Technology Center, Hangzhou Liqun Environmental Protection Paper Co., Ltd., Hangzhou, 310018, China
[d] Department of Chemical and Biological Engineering, Center for Biotechnology and Interdisciplinary Studies, Rensselaer Polytechnic Institute, Troy, NY, 12180, USA

ARTICLE INFO

*Keywords:*
Nicotine degradation
*Pseudomonas* sp. JY-Q
Homologous dehydrogenase
Comparative characterization

ABSTRACT

Nicotine contamination in tobacco waste effluent (TWE) from tobacco industry is a serious threat to public health and environment. Microbial degradation is an impending approach to remove nicotine and transform it into some other high value chemicals. *Pseudomonas* sp. JY-Q exhibits high efficiency of degradation, which can degrade 5 g/L of nicotine within 24 h. In strain JY-Q, we found the co-occurrence of two homologous key enzymes NicA2 and Nox, which catalyze nicotine to *N*-methylmyosmine, and then to pseudooxylnicotine via simultaneous hydrolysis. In this study, recombinant NicA2 and Nox were expressed in *E. coli* BL21(DE3) and purified. *In vitro*, the activity of recombinant NicA2 and Nox was accelerated by adding co-factor $NAD^+$, suggesting that they worked as dehydrogenases. The optimal reaction conditions, substrate affinity, catabolism efficiency, pH-stability and thermal-stability were determined. Nox showed lower efficiency, but at a higher stability level than NicA2. Nox exhibited wider pH range and higher temperature as optimal conditions for the enzymatic reaction. In addition, The Nox showed higher thermo-stability and acid-stability than that of NicA2. The study on enzymatic reaction kinetics showed that Nox had a lower *K*m and higher substrate affinity than NicA2. These results suggest that Nox plays more significant role than NicA2 in nicotine degradation in TWE, which usually is processed at low pH (4–5) and high temperature (above 40 °C). Genetic engineering is required to enhance the affinity and suitability of NicA2 for an increased additive effect on homologous NicA2 and Nox in strain JY-Q.

## 1. Introduction

Nicotine in tobacco waste effluent (TWE) is a principal contaminant of the ecological environment, together with a predominant addictive and toxic constituent in cigarette. Nicotine degradation by bacteria is a potential strategy for environmental remediation [1–3], and the process can produce some other high value metabolites [4,5]. Three nicotine metabolism pathways: pyrrolidine, pyridine, variant of the pyridine and pyrrolidine (Vpp), in *Pseudomonas*, *Arthrobacter*, and *Ochrobactrum* species [6–12], respectively, have been reported. The main difference of initial procedures between pyrrolidine and pyridine pathways is the dehydrogenation/oxidization sites on pyrrolidine or pyridine loop of nicotine [11,13,14]. The pyrrolidine pathway comprised of three functional modules, Nic1, Spm, and Nic2, response for nicotine transformation to maintain energy productivity and metabolite/nutrition acquisition [15].

NicA2 and Nox are nicotine dehydrogenases in the pyrrolidine pathway and have been identified from *Pseudomonas putida* S16 [6,16] and *Pseudomonas* sp. HZN6 [17]. The co-occurrence of NicA2 and Nox in JY-Q was identified in our previous study [18]. As shown in Fig. 1A and B, NicA2 and Nox catalyze nicotine into *N*-methylmyosmine, and then simultaneously transform into pseudooxynicotine through tautomerization and hydrolysis [17,19,20]. For the determination of further catalytic properties characterization, NicA2 from strain S16 has been expressed in *E. coli* [1,21]. The protein structure analysis revealed that NicA2 from strain S16 has several highly conserved amino acid residues,

* Corresponding author.
** Corresponding author.
*E-mail addresses:* Yangy@zjtobacco.com (Y. Yang), whzhong@zjut.edu.cn (W. Zhong).

https://doi.org/10.1016/j.pep.2020.105767
Received 8 June 2020; Received in revised form 16 September 2020; Accepted 19 September 2020
Available online 26 September 2020

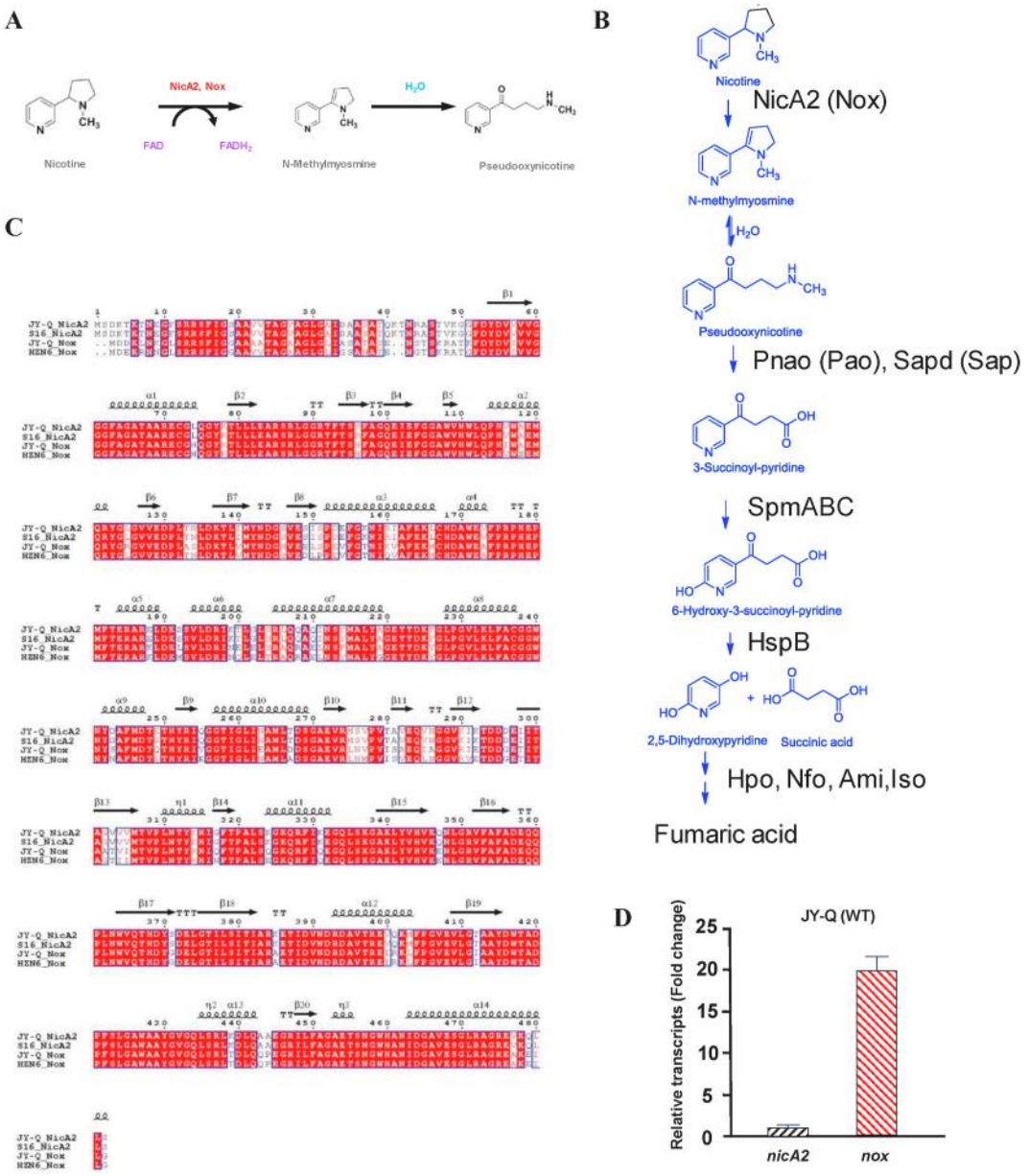


**Fig. 1. Catalysis mechanism and sequence alignment for NicA2 and Nox. (A)** Proposed working model of nicotine transformation catalyzed by NicA2 and Nox. **(B)** Pyrrolidine pathway for nicotine degradation. **Nic1**: NicA2 (Nox), Pnao (Pao) and Sapd (Sap); **Spm** and **Nic2**: Hpo, Nfo, Ami and Iso were included in this schema. **(C)** Multiple alignment for amino acid sequences of S16_NicA2, HZN6_Nox, JY-Q_NicA2 and JY-Q_Nox. **(D)** Relative transcriptional levels for *nicA2* and *nox* in strain JY-Q under BSM culture supplemented with 1.0 mg/mL nicotine, examined by RT-qPCR with 16S rRNA as internal reference. α-helix and β-strand of protein secondary structures were respectively flagged by squiggles and arrows. The identical and similar residues were denoted by red and hollow boxes, respectively. HspB, 6-hydroxy-3-succinoylpyridine (HSP) hydroxylase; Iso, maleate isomerase; Nfo, *N*-formylmaleamic acid (NFM) deformylase; Hpo, 2,5-dihydroxy-pyridine (2,5-DHP) dioxygenase; Ami, maleamate amidase; Nox, nicotine oxidase; Pao, pseudooxynicotine amine oxidase; Sap, NADP + -dependent 3-succinoylsemialdehyde-pyridine (DSP) dehydrogenase; NicA2, nicotine oxido-reductase; Pnao, pseudooxynicotine amine oxidase; Sapd, DSP dehydrogenase; Spm, 3-succinoyl-pyridine (SP) monooxygenase.

such as W427 and N462 (for flavin (FAD) binding) [22] and T381 (for substrate recognition) [23]. Nox in strain JY-Q (478 aa) exhibited 80.7%, 82.1%, and 91.8% sequence identities to NicA2 (482 aa) from strain S16, NicA2 (482 aa in length) from strain JY-Q, and Nox (478 aa) from strain NZN6, respectively [Fig. 1C].

In our previous study, we found the homologous genes of NicA2 and Nox contribute to nicotine degradation at different levels [15]. First, when *nox* and *nicA2* were deleted from the genome of wild type strain JY-Q, the mutant Δ*nox* was less efficient than the mutant Δ*nicA2*. This result suggested that the contribution of Nox was higher than that of NicA2. Secondly, the *nox* transcription intensity was found to be about 20–fold higher than that of *nicA2* [15] [Fig. 1D]. Finally, when *nox* and *nicA2* both were deleted, the mutant Δ*nicA2, nox* could not grow on nicotine as sole carbon/nitrogen sources, suggesting that these two genes are absolutely indispensable for nicotine utilization in strain JY-Q. When the mutant Δ*nicA2, nox* was complemented with *nox* and *nicA2*, respectively, the complemented strains Δ*nicA2,nox-nicA2C* (supplemented with *nicA2*) and Δ*nicA2,nox-noxC* (supplemented with *nox*) both recovered the ability for nicotine degradation. The difference in the contribution of NicA2 and Nox may result from their sequence variants (82% identity) [Fig. 1C]. The goal of current study is to confirm this hypothesis, requiring additional insight into the characteristics of the

**Table 1**
Strains, plasmids and primers used in this study.

| Strains | | |
|---|---|---|
| *Pseudomonas* sp. JY-Q | | Biodegrader to transform 5 g/L nicotine during 24 h |
| *Escherichia coli* BL21 | | *E. coli* BL21 (DE3), a protein expression host |
| BL21-pET-28a(+)-*nicA2* | | BL21(DE3) with pET28a-*nicA2* |
| BL21-pET-28a(+)-*nox* | | BL21(DE3) with pET28a-*nox* |
| **Plasmids** | | |
| pET-28a(+) | | T7-driven expression vector, $Km^R$ |
| pET-28a(+)-*nicA2* | | *nicA2* in *BamH* I and *Hind* III sites of pET28a |
| pET-28a(+)-*nox* | | *nox* in *BamH* I and *Hind* III sites of pET28a |
| **Primers** | | |
| Genes | Primer Name | Primer Sequence (5′-3′) |
| *nicA2* | *nicA2*-Forward | CAGCAAATGGGTCGC**GGATCC**ATGTATAACGACGGAAGCGT |
| | *nicA2*-Reverse | CTCGAGTGCGGCCGC**AAGCTT**CTAGCTTAAGAGCTGCTTAACCTCC |
| *nox* | *nox*-Forward | CAGCAAATGGGTCGC**GGATCC**ATGGATGACAAACTAAACAAAGGCC |
| | *nox*-Reverse | CTCGAGTGCGGCCGC**AAGCTT**TTAACCTAATATTTCTTTCGCTTCGC |

Note: '—', restriction cleavage site.

two homologous enzymes, Nox and NicA2. The investigation includes: (1) the expression of recombinant Nox and NicA2 in *E. coli*; and (2) the determination and comparison of the enzymatic characteristics of the recombinant Nox and NicA2.

## 2. Materials and methods

### 2.1. Strains, plasmids, chemicals and culture media

Strain *Pseudomonas* sp. JY-Q (CCTCC No. M2013236) was isolated from tobacco waste extract (TWE). The *nicA2* and *nox* genes were cloned from *Pseudomonas* sp. JY-Q, which has capability of degrading nicotine (5 mg/L) in 24 h. Plasmid minikit was purchased from Axygen Scientific Inc. (Hangzhou, China). The *E. coli* BL21(DE3) was purchased from Novagen (Shanghai, China). The *E. coli* BL21(DE3)/pET-28a(+)-*nicA2* and *E. coli* BL21(DE3)/pET-28a(+)-*nox* were constructed in our laboratory [Table 1].

Nicotine (99%) was purchased from FlukaChemie GmbH (Buchs Corp., Switzerland); $NAD^+$ (nicotinamide adenine dinucleotide) was purchased from Sangon Biotech Co., Ltd. (Shanghai, China). Oligonucleotides synthesis and DNA sequencing were carried out at Tsingke Biotechnology Col., Ltd. (Hangzhou, China). The induction reagent IPTG (isopropyl-β-D-thiogalactopyranoside) was obtained from Beijing Solarbio Science & Technology Co., Ltd. (Beijing, China).

Luria-Bertani (LB) broth composition: Yeast extract 5 g, tryptone 10 g, NaCl 10 g up to 1 L with $ddH_2O$. BSM (basic salt medium) was prepared as follows: $Na_2HPO_4$ 5.57 g, $CaCl_2$ 0.001 g, $KH_2PO_4$ 2.44 g, $FeCl_3{\cdot}6H_2O$ 0.001 g, $K_2SO_4$ 1 g, $MnCl_2{\cdot}4H_2O$ 0.0004 g, $MgCl_2{\cdot}6H_2O$ 0.2 g, and $ddH_2O$ 1000 mL. 0.1 g/L nicotine were added into this culture as sole carbon/nitrogen source. Unless otherwise stated, a shaking speed of 180 rpm was the default condition for cultures. Cell optical density ($OD_{600}$) for bacterial growth was detected by spectrophotometer (UV1000, Shanghai Tianmei Instrument Col. Ltd., China).

### 2.2. Construction and identification of the recombinant E. coli BL21 harboring nicA2 and nox

The genes of *nicA2* and *nox* were cloned from the genomic DNA of strain JY-Q by PCR using EasyPfu DNA polymerase and specific primers [Table 1]. PCR product was digested at *BamH* I and *Hind* III sites using corresponding restriction endonucleases and inserted into the pET-28a vector (His-tag in *N*-terminus). The resultant recombinant vector was transferred into *E. coli* BL21 (DE3) using heat shock transformation method. The final target cells harboring *nicA2* and *nox*, *E. coli* BL21 (DE3)/pET-28a-*nicA2* and *E. coli* BL21 (DE3)/pET-28a-*nox*, were screened on medium containing 50 mg/L kanamycin.

Recombinant *E. coli* BL21 harboring *nicA2* and *nox* (2% inoculation volume, v/v) were, respectively, inoculated into 250 mL LB medium containing 50 μg/L kanamycin and incubated at 37 °C and 180 rpm. After overnight culture, the broth was inoculated into fresh LB medium containing 50 μg/L of kanamycin. When the $OD_{600}$ of the broth reached 0.6, 0.5 mM IPTG was added to induce the expression of NicA2 and Nox by the recombinant strains, which were then cultured at 16 °C and 180 rpm for 16 h. The induced host cells were harvested by centrifugation at 8000 rpm for 20 min at 4 °C. After washing, PBS buffer was used to suspend the cells and adjusted the final cell density to an identical $OD_{600}$ value.

The cell suspension was stored at 4 °C for 24 h to synchronize status of the resting cells for functional identification. The synchronized resting cells were inoculated into a PBS containing 1.0 mg/mL nicotine, and then incubated under 37 °C to measure its ability to degrade nicotine. Meanwhile, BL21/pET-28a(+) [strain BL21 bearing the pET-28(+) vector] was used as the negative control.

### 2.3. Expression, purification, and function identification of NicA2 and Nox

After culture and induction with IPTG according to the method 2.2, the induced host cells were harvested by centrifugation at 8000 rpm for 5 min at 4 °C. After washing three times with saline, cells were suspended in 30 mL binding buffer (20 mM Tris-base, 0.5 M NaCl and 10 mM imidazole). The suspensions were transferred to 50 mL beaker within an ultrasonic disintegrator (VCX500, Sonics & Materials, Inc., USA) operated at 250 W (5 min, 3 s ultrasonic time, 3 s interval time). All suspensions were kept in an ice bath during the ultrasonic process to prevent heating. The resultant supernatant (30 mL) was collected by centrifugation at 12,000 rpm for 20 min at 4 °C. Sediment was processed by 10 mL denaturation solution (20 mM Tris-base, 0.5 M NaCl, 10 mM imidazole, and 6 M urea) to acquire target proteins in inclusion bodies.

His-tagged NicA2 and Nox, were purified and eluted by using affinity chromatography with 1 mL Ni-NTA (Nickel-nitrilotriacetic acid) resin and appropriate imidazole. After sample loading, 5 mL binding buffer was used to wash the column to remove non-target proteins. The specific protein elution was carried out by gradually adding elution buffer (20 mM Tris-base, 0.5 M NaCl and 0.5 M imidazole). Protein molecular weights of these two His-tagged proteins were then assessed by SDS-PAGE. The protein concentration was identified by the BCA (Bicinchoninic acid) assay (Cat# GK5021, Generay, China). The nicotine-degrading activities of the enzymes were measured in a reaction mixture of PBS containing 1.0 mg/mL nicotine under optimal temperature and pH.

### 2.4. Determination of the optimal reaction conditions for recombinant NicA2 and Nox

The optimal pH of the recombinant NicA2 and Nox were determined

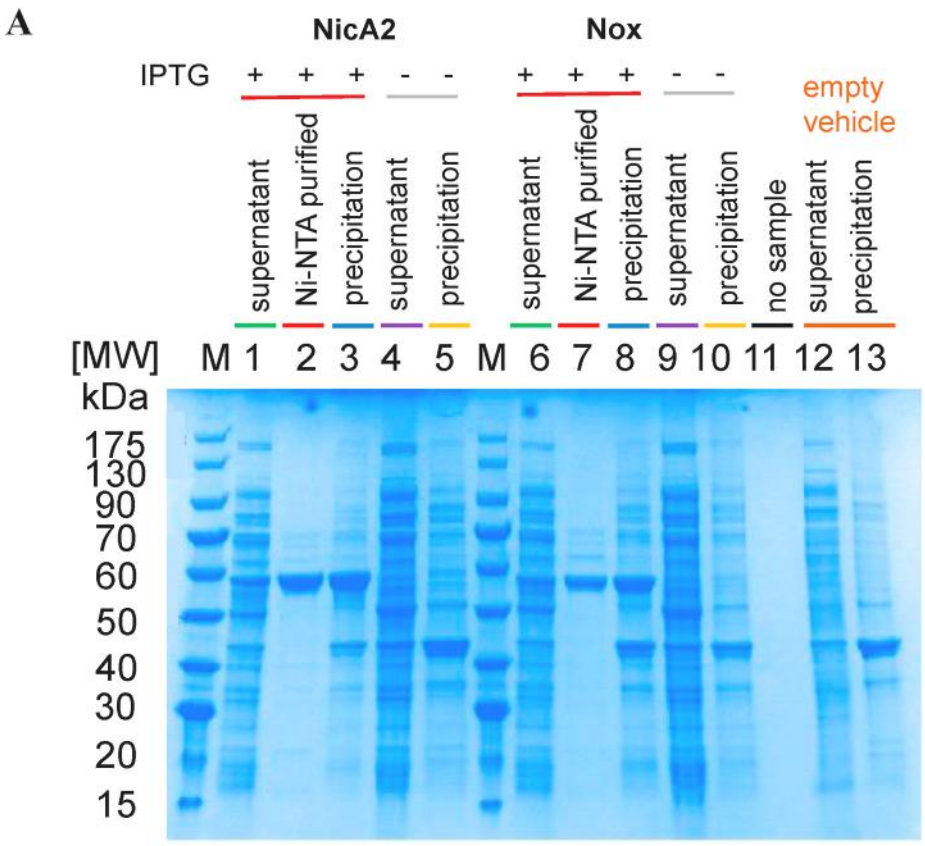


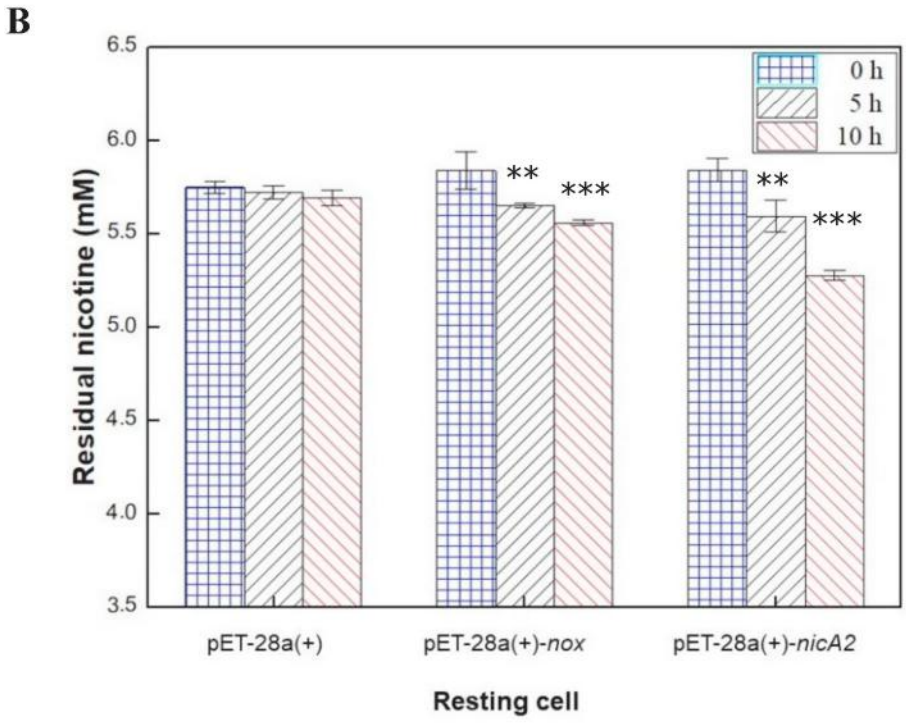


**Fig. 2. Expression and functional of NicA2 and Nox. (A)** SDS-PAGE analysis of the expressed and purified recombinant NicA2 and Nox. M, protein marker. Lane 1, supernatant after cell disruption from the BL21/pET-28a(+)-*nicA2* with IPTG induction. Lane 2, purified NicA2 by Ni-NTA. Lane 3, precipitation after cell disruption from the BL21/pET-28a(+)-*nicA2* with IPTG induction. Lane 4, supernatant after cell disruption from the BL21/pET-28a(+)-*nicA2*. Lane 5, precipitation after cell disruption from the BL21/pET-28a(+)-*nicA2*. Lane 6, supernatant after cell disruption from the BL21/pET-28a(+)-*nox* with IPTG induction. Lane 7, purified Nox by Ni-NTA. Lane 8, precipitation after cell disruption from the BL21/pET-28a(+)-*nox* with IPTG induction. Lane 9, supernatant after cell disruption from the BL21/pET-28a(+)-*nox*. Lane 10, precipitation after cell disruption from the BL21/pET-28a(+)-*nox*. Lane 11: no sample, to separate negative groups (Lane 12–13, empty vector) from above (Lane 1–10). Lane 12, supernatant after cell disruption from the BL21/pET-28a(+). Lane 13, precipitation after cell disruption from the BL21/pET-28a(+). MW: molecular weight. **(B)** Nicotine degrading by resting cells of recombinant BL21/pET-28a(+) harboring *nicA2* or *nox*,.: **, $p$-value < 0.01; ***, $p$-value < 0.001, ANOVA, compared to control.

in a reaction system containing 0.1 mg NicA2 or Nox, and 1000 μL of 100 mM NaAc-HAc (pH 5.0–6.0), 100 mM PBS (pH 6.0–8.0), and 100 mM Tris-HCl (pH 8.0–9.0), respectively. After 6 h reaction under 37 °C, enzymes were inactivated in a 100 °C water bath for 5 min. The residual nicotine was examined using HPLC.

The optimal temperature of the recombinant NicA2 and Nox were determined in the reaction system under the optimal pH and a temperature ranging from 20 to 45 °C reaction with a stepwise increase of 5 °C.

**Table 2**
Purification of NicA2 and Nox enzymes.

| Sample[a] | | Total protein (mg) | Total activity (U)[b] | Specific activity (U/mg protein) | Purification (fold)[c] | Yield (mg/g DCW)[d] |
|---|---|---|---|---|---|---|
| NicA2 | Crude | 42.1 | 39.0 | 0.92 | – | 63.6 |
| | Ni-NTA purified | 6.28 | 35.7 | 5.68 | 6.14 | |
| Nox | Crude | 36.7 | 19.9 | 0.54 | – | 70.9 |
| | Ni-NTA purified | 4.43 | 13.5 | 3.04 | 5.59 | |

Note.
[a] The total volume for crude lysates and Ni-NTA purified enzymes is 30 mL and 5 mL, respectively.
[b] One unit of enzyme activity is defined as the amount of enzyme required to consume 1 nmol of nicotine per minute under the assay conditions.
[c] $purification\ fold = \frac{specific\ activity\ of\ purified\ enzymes}{specific\ activity\ of\ crude\ lysates} \times 100\%$
[d] DCW (dry cell weight) is calculated based on a calibration curve between optical density (OD) and dry cell weight of *E. coli*. The cell yield of *E. coli* BL21/pET-*nicA2* and *E. coli* BL21/pET-*nox* in 200 mL broth reached about 98.7 mg and 62.5 mg, respectively.

### 2.5. Determination of the thermal- and pH- stability of recombinant NicA2 and Nox

Stability of recombinant NicA2 and Nox under varied pH was examined in a solution containing appropriately diluted enzymes in different buffers: citrate buffer (pH 3.0–6.5), PBS (pH 6.0–8.0), Tris-HCl (pH 7.5–9.0), and Gly-NaOH (pH 8.5–10.0), respectively. After maintaining at 35 °C for 2 h, the solution was then sampled and transferred into a mixture system containing nicotine with optimal pH buffer for a 6 h enzymatic reaction. The residual nicotine was then measured using HPLC to determine their remaining activity for nicotine degradation.

Diluted enzymes were pre-incubated at 60 °C and sampled at an interval time of 10 or 20 min, respectively, to determine the thermal-stability of recombinant NicA2 and Nox. The residual enzymatic activity of the samples was measured in a reaction mixture. After 6 h reaction at 35 °C, the residual nicotine in samples was measured using HPLC to determine their remaining activity for nicotine degradation. The original activity of NicA2 and Nox (0 min) without incubation was defined as control.

### 2.6. Kinetic parameter determination

The kinetic parameters of NicA2 and Nox were determined in the reaction mixtures (1000 μL) containing 0.25 mg/mL NicA2 or Nox, 1.0 mg/mL $NAD^+$ as the co-factor, and 0.02, 0.03, 0.04, 0.05, 0.075, 0.1, 0.25, 0.5 and 1.0 mg nicotine as substrate. The variant concentration nicotine solutions were prepared by serial dilution with $Na_2H$-$PO_4$–$NaH_2PO_4$ buffer (100 mM, pH 7.0). The residual nicotine was examined using HPLC after 0.5–1 h reaction under optimal conditions. All reactions were performed in triplicate.

Kinetic parameters were calculated based on the following equation: $v = v_{max}[S]/([S] + Km)$, Where [S] is the varied concentration of the substrate and $v_{max}$ is the maximum reaction velocity.

### 2.7. Analytical and statistical methods

Nicotine was measured with HPLC (Agilent 1260 series). An Agilent SB-C18 column (4.6 × 150 mm) was attached to a high-performance liquid chromatography (HPLC) system, and the detector wavelength was set at 254 nm. The retention time of nicotine was about 2.3 min based on the standard [18]. The mobile phase consists of 0.1 M $KH_2PO_4$ (pH 3.0) and methanol at volumetric ratio of 90:10 (v/v), and run at a flow rate of 1 mL/min. The initial concentration of nicotine ($C_0$) and its remaining concentration ($C_t$) at t hours were both recorded. The concentration of residual nicotine in the reaction system was inferred by HPLC peak area at the expected retention time. All experiments were conducted in triplicate, and BSM with no inoculation was taken as the negative control [10,24].

NADH concentration was detected using WST-8 based colorimetric approaches with necessary modification (NicA2/Nox replaced dehydrogenases, NAD+/NADH Assay Kit, Beyotime, China), to determine stoichiometry ratio for nicotine and $NAD^+$.

All data are presented as the mean ± standard error (SE). Data analysis was carried out by the Origin 9.1 program (OriginLab Corp., Northampton, MA, USA). In this study, at least three independent replicates were conducted.

### 2.8. Bioinformatics analysis

NicA2 from *P. putida* S16 and Nox from *Pseudomonas* sp. HZN6 as prototypes were acquired from NCBI. For multiple sequence alignment, S16_NicA2, HZN6_Nox, JY-Q_NicA2, JY-Q_Nox sequences were introduced into MUSCLE [25], and resultant visualization was conducted by ESPript3 (available at espript.ibcp.fr/ESPript). Identical residues were denoted by red background boxes. Variable and similar amino acid residues are labeled in black and orange, respectively. A comparative scheme of two enzymatic structures was prepared by PyMOL (DeLano Scientific LLC, template S16_NicA2 PDB code: 5TTJ).

NicA2 and Nox sequences were submitted into NCBI BLAST [26] against RefSeq [27] to acquire their candidate homologs. Subsequently, their genomic contexts were manually curated, considering the functional relatedness amongst Nic1-Spm-Nic2. The contextual information of *nicA2* and *nox*–like homologs was investigated by the VRprofile suite [28]. Phylogeny of these protein sequences was generated by MEGA 7, with the NJ method and the JTT substitution model as well as 1000 bootstraps [29].

## 3. Results

### 3.1. Construct and identify the recombinant E. coli BL21/pET-nicA2 and BL21/pET-nox

The recombinant BL21 harboring *nicA2* or *nox, E. coli* BL21/pET-*nicA2* and *E. coli* BL21/pET-*nox* were successfully constructed. As shown in Fig. 2A, the target proteins were expressed as soluble forms. However, the recombinant BL21 harboring *nicA2* or *nox* could not grow well in BSM supplemented with nicotine, the efficiency of nicotine removal was also not sufficiently high to be detectable (Data not shown). These results may result from that the recombinant BL21 harboring *nicA2* or *nox,* lacking the successive metabolic enzymes encoded by *pnao* (*pao*) and *sapd* (*sap*) to transform pseudooxynicotine [Fig. 1B]. A similar phenomenon had been previously observed in strain KT2440 carrying *nox* (KT-*nox*), which also exhibited a long lag phase for their nicotine degradation and individual growth [17,20].

Thus, nicotine removal efficiency of the resting cells of recombinant BL21 was measured with a large quantity of cells. The synchronized resting cells exhibited significant nicotine removal. Compared to the control group (BL21-pET-28a(+)) without effect, the groups BL21-pET-28a(+)-*nicA2* and BL21-pET-28a(+)-*nox* both showed significant decrease of nicotine content from about 6.16 mM to 5.61 mM (5.30 mM) and 5.67 mM (5.54 mM), respectively, after 5 h (10 h) reaction [Fig. 2B]. NicA2 and Nox both were expressed and exhibited the activity of nicotine removal in recombinant cells without significant ability difference. Thus, it is necessary to acquire and compare their *in vitro* enzymatic characteristics of NicA2 and Nox.

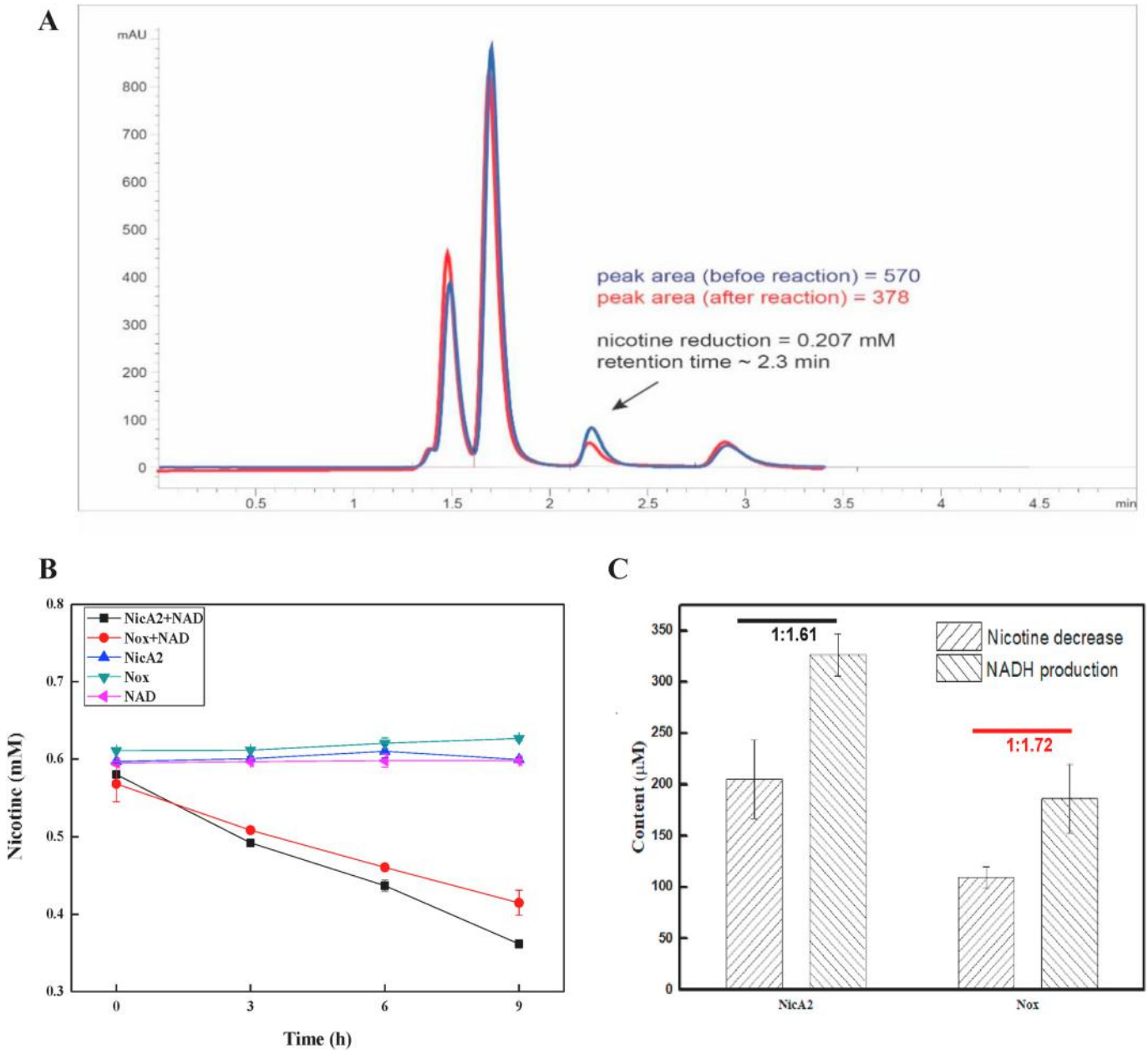


**Fig. 3. The NAD$^+$effects on nicotine elimination in the reaction mixture**. **(A)** HPLC assay for residual nicotine in the reaction system. Residual nicotine samples were retrieved from the 0 h (blue) and 12 h (red) reaction treated by Nox. **(B)** Additional NAD$^+$ could obviously facilitate nicotine reduction by NicA2 and Nox if encountering the excessive amount of nicotine. No nicotine reduction was observed if no NAD$^+$ was added into the NicA2/Nox reaction system. (**C**) The spectrophotometric assay for nicotine transformation and NADH yield.

### *3.2. Expression, purification, and function identification of NicA2 and Nox*

After culture and IPTG induction, the final broth $OD_{600}$ of *E. coli* BL21/pET-*nicA2* and *E. coli* BL21/pET-*nox* in 200 mL media reached 3.95 and 2.50, respectively. Based on a calibration curve between OD and dry cell weight of *E. coli*, the cell yield of *E. coli* BL21/pET-*nicA2* and *E. coli* BL21/pET-*nox* in 200 mL broth reached about 98.7 mg and 62.5 mg. All cells were harvested and then transferred into 30 mL binding buffer for disruption by sonication and subsequent centrifugation. The resultant supernatants (30 mL) and sediments were further used to prepare purified proteins.

As shown in Fig. 2A, the target proteins were expressed as soluble forms by the recombinant BL21 harboring *nicA2* or *nox, E. coli* BL21/pET-*nicA2* and *E. coli* BL21/pET-*nox*. The target proteins, His-tagged NicA2 and Nox, were then purified and eluted by using affinity chromatography with 1 mL Ni-NTA (Nickel-nitrilotriacetic acid) resin and the appropriate concentration of imidazole. The specific protein eluent was collected for desalination by 3.6 kDa dialysis, the final purified recombinant NicA2 and Nox solutions were then stored directly or after lyophilization. SDS-PAGE gel results also showed that the target proteins were successfully purified. The molecular masses (MW) of the recombinant NicA2 and Nox indicated by SDS-PAGE, 56.1 kDa and 55.7 kDa respectively, were the accurate size for His-tagged NicA2 and Nox. The electrophoresis estimations of MW were consistent with the theoretical size of NicA2 (54 kDa) and Nox (53 kDa) [Fig. 2A].

The molar concentration normalization of the enzymes obtained was determined through a series of PBS gradient dilutions to prepare the reaction system, to directly compare the efficiency of nicotine removal by these two isozymes. After purification using Ni-NTA resin, 5 mL of

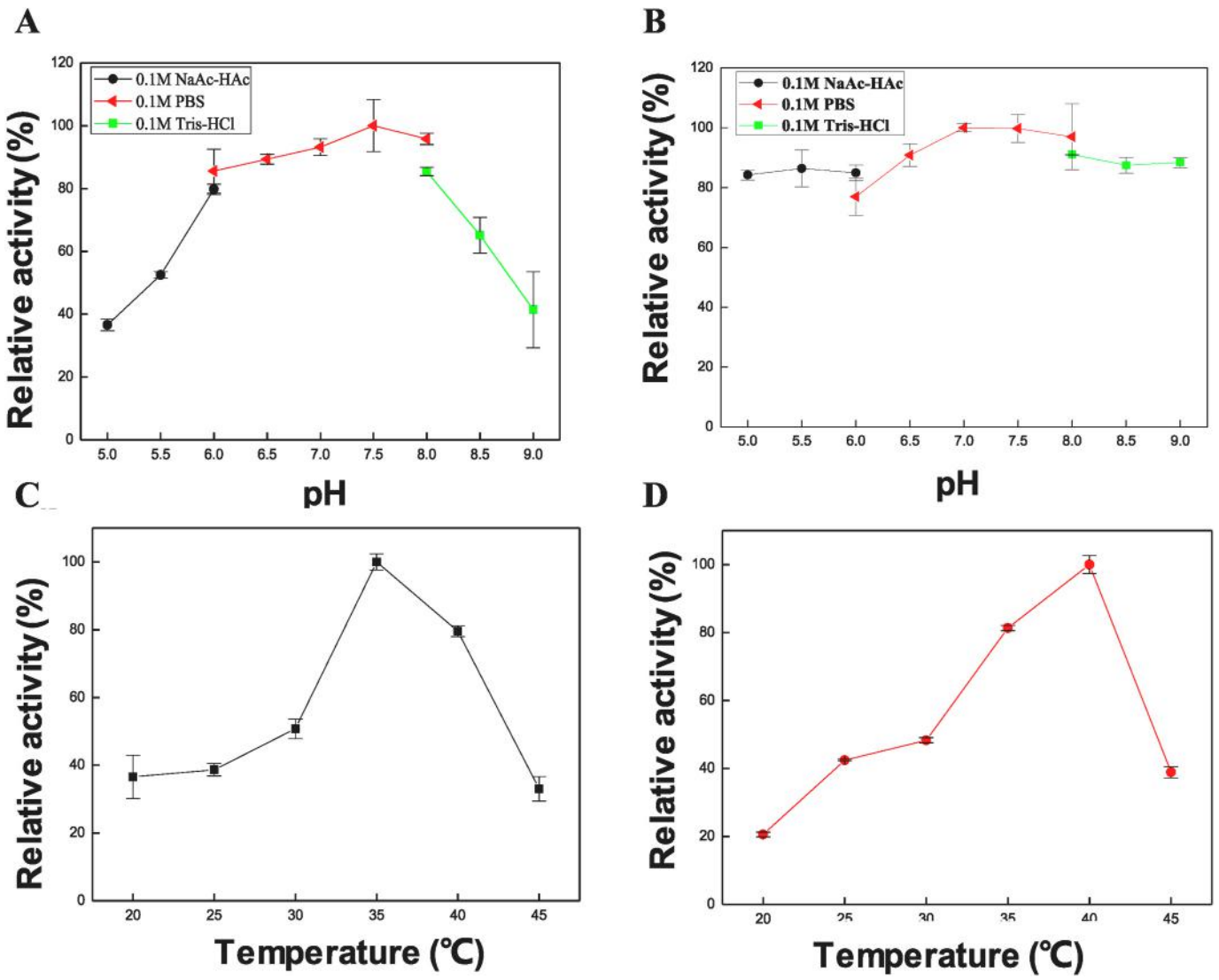


**Fig. 4. Optimal pH (A–B) and temperature (C–D) conditions for NicA2 and Nox.**

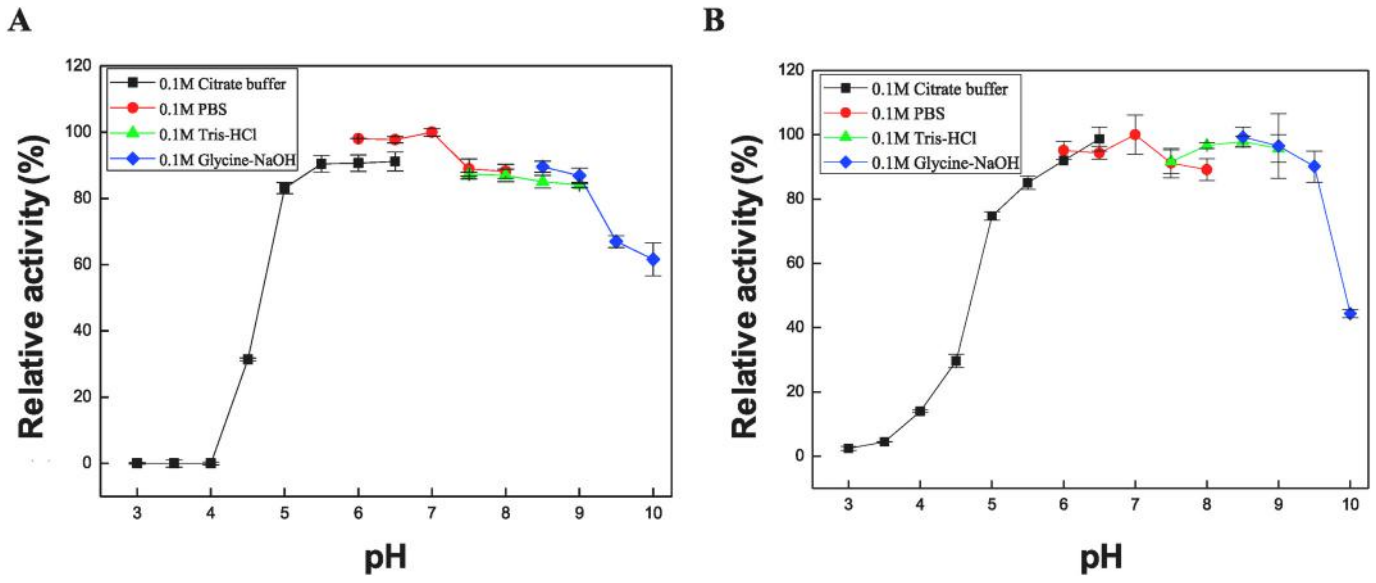


**Fig. 5. Stability analysis under pH changes for NicA2 (A) and Nox (B).**

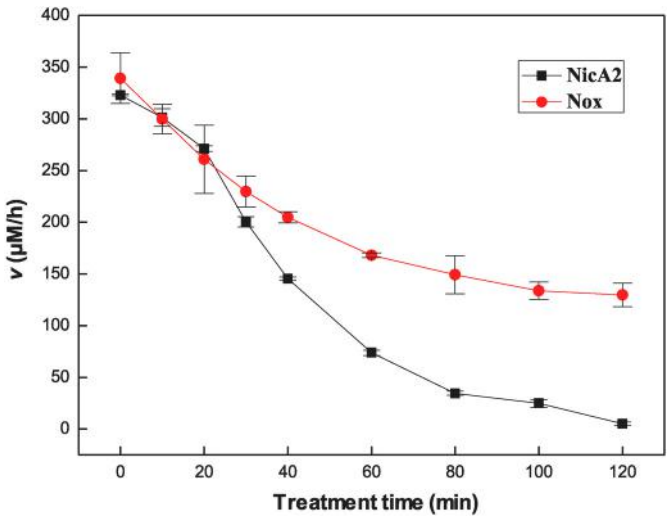


**Fig. 6.** Thermal stability analysis for NicA2 and Nox.

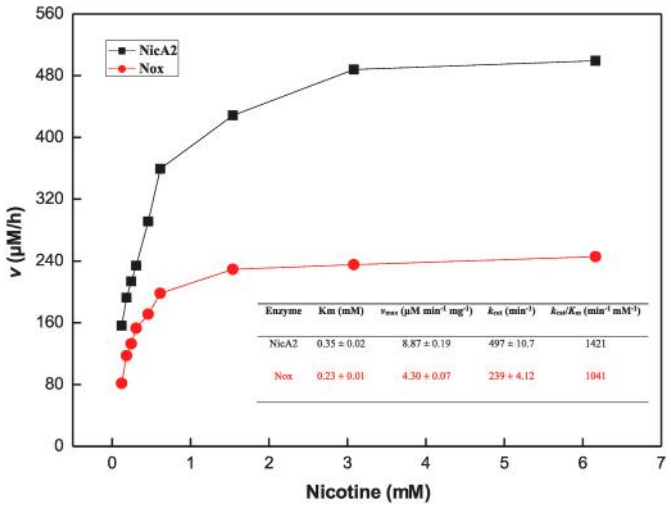


**Fig. 7.** Kinetics curves for NicA2 and Nox.

NicA2 (1.26 mg/mL) and Nox (0.89 mg/mL) were each prepared from about 30 mL supernatant of cell suspension after disruption by sonication. In addition, 5 mL NicA2 (0.79 mg/mL) and 2 mL Nox (0.47 mg/mL) were acquired from inclusion bodies. The yield of purified recombinant NicA2 and Nox expressed in strain BL21 is 63.6 mg and 70.9 mg per gram dry cell weight, respectively, while the purification efficiency for recombinant NicA2 and Nox was about 6-fold [Table 2].

The purified NicA2 and Nox from *E. coli* were tinted yellow indicating they are flavoproteins with FAD (Flavin) bound either covalently or tightly. Nicotine-degrading activity and its mechanism of purified proteins were measured in a reaction mixture of PBS containing 1.0 mg/mL nicotine under optimal temperature and pH. However, no significant nicotine reduction was observed if no $NAD^+$ was added into the reaction mixture (containing 0.1 mg/L nicotine mixed with 0.1 mg NicA2/Nox). In addition, no nicotine reduction was observed when FAD was added into the reaction mixture [Fig. 3A and B]. These results suggested that NicA2 and Nox seemed to work as dehydrogenases, in agreement with the previous finding that additional FAD/FMN did not accelerate nicotine degradation by recombinant NicA2 from strain S16 [21]. A simple spectrophotometric assay was conducted to detect nicotine reduction and NADH production for 6 h to measure the reaction stoichiometry. The ratio of nicotine decrease and NADH yield of NicA2 and Nox reached 1:1.61 and 1:1.72, respectively. These values are close to the theoretical equivalent 1:2 if only $NAD^+$ is the *in vitro* recipient of nicotine dehydrogenation. Moreover, we also found the amount of nicotine reduction catalyzed by Nox is less than by NicA2 [Fig. 3C]. Collectively, these findings indicate that nicotine dehydrogenation by NicA2 and Nox can be facilitated by the additional $NAD^+$ as the hydrogen recipient.

### 3.3. Optimal reaction conditions of recombinant NicA2 and Nox

As shown in Fig. 4, the optimal pH of NicA2 was 7.5, while that of Nox was 7.0–7.5. However, the relative activity of Nox remained at a higher level (above about 80%) than that of NicA2 (above about 35%), when pH varied from 5.0 to 9.0. We conclude that NicA2 and Nox are nicotine dehydrogenases with good environmental pH adaptabilities (especially for Nox). Moreover, a wider pH range was observed for Nox. These two isozymes might be resistant to intracellular acid accumulation during pollutant degradation, especially for Nox. Specifically, NicA2 at pH 7.5 had the best ability to eliminate nicotine (364 μM $h^{-1}$) and Nox at pH 7.0 eliminated nicotine at 340 μM $h^{-1}$ [Fig. 4 A, B].

As shown in Fig. 4C and D, the optimal temperature of NicA2 was 35 °C, while that of Nox was 40 °C, with a catalyzing velocity of 411 μM $h^{-1}$ and 328 μM $h^{-1}$, respectively. NicA2 activity was still higher than that of Nox, suggesting that NicA2 was more suitable for nicotine degradation than Nox under optimal conditions. In contrast to this observation, strain JY-Q was found to prefer Nox to undertake the major role of nicotine transformation. The explanation of this unlikely phenomenon could be associated with genetic contexts and enzymatic features of *nicA2* and *nox*. Thus, we examined their thermo-stability and acid-tolerance.

### 3.4. Thermal stability and acid-tolerance of recombinant NicA2 and Nox

After maintaining at different pH values at 35 °C for 2 h, the residual enzyme activity was measured. As shown in Fig. 5, the NicA2 activity (catalyzing velocity is 293 μM $h^{-1}$) and the Nox activity (catalyzing velocity is 260 μM $h^{-1}$) after maintaining at pH 7.0 for 2 h was set at '100%' activity, respectively. If the pretreated pH was less than 4, the NicA2 activity decreased to zero, while the Nox activity remained 4.5–14.0%. In summary, Nox could be a more acid–tolerant isozyme and is more appropriate to be deployed by JY-Q for acid accumulation during pollutant degradation.

After dilution enzymes of the recombinant NicA2 and Nox were pre-incubated at 60 °C, the initial and residual enzymatic activity of the samples was measured in a reaction mixture. As shown in Fig. 6, the initial enzymatic reaction velocity (denoted as 0 min) was 323 μM $h^{-1}$ and 340 μM $h^{-1}$ for NicA2 and Nox, respectively. The residual enzymatic activity of NicA2 decreased more sharply than that of Nox when treated at increased temperature. The residual enzymatic activity of NicA2 at 35 min was 50% of its initial activity, i.e., its half-life value ($t_{1/2}$) was 35 min. However, the residual enzymatic activity of Nox after 120 min treatment was 38% of its initial activity.

In conclusion, NicA2 seems to have lost the majority of catalytic ability at high temperature, while Nox activity still showed detectable activity even after 120 min treatment, indicating its outstanding thermostability.

### 3.5. Comparison of reaction kinetics between recombinant NicA2 and Nox

In our previous study, the transcriptional level of *nicA2* was lower than that of *nox* in strain JY-Q. It seemed that Nox was utilized by JY-Q prior to NicA2 for nicotine degradation, suggesting a potential difference of reaction kinetics between NicA2 and Nox. Thus, the reaction kinetics of recombinant NicA2 and Nox was determined.

As shown in Fig. 7, the catalytic kinetics properties of NicA2, especially the substrate affinity and reaction maximum velocity, were significantly different from those of Nox. The $K_m$ values of NicA2 and

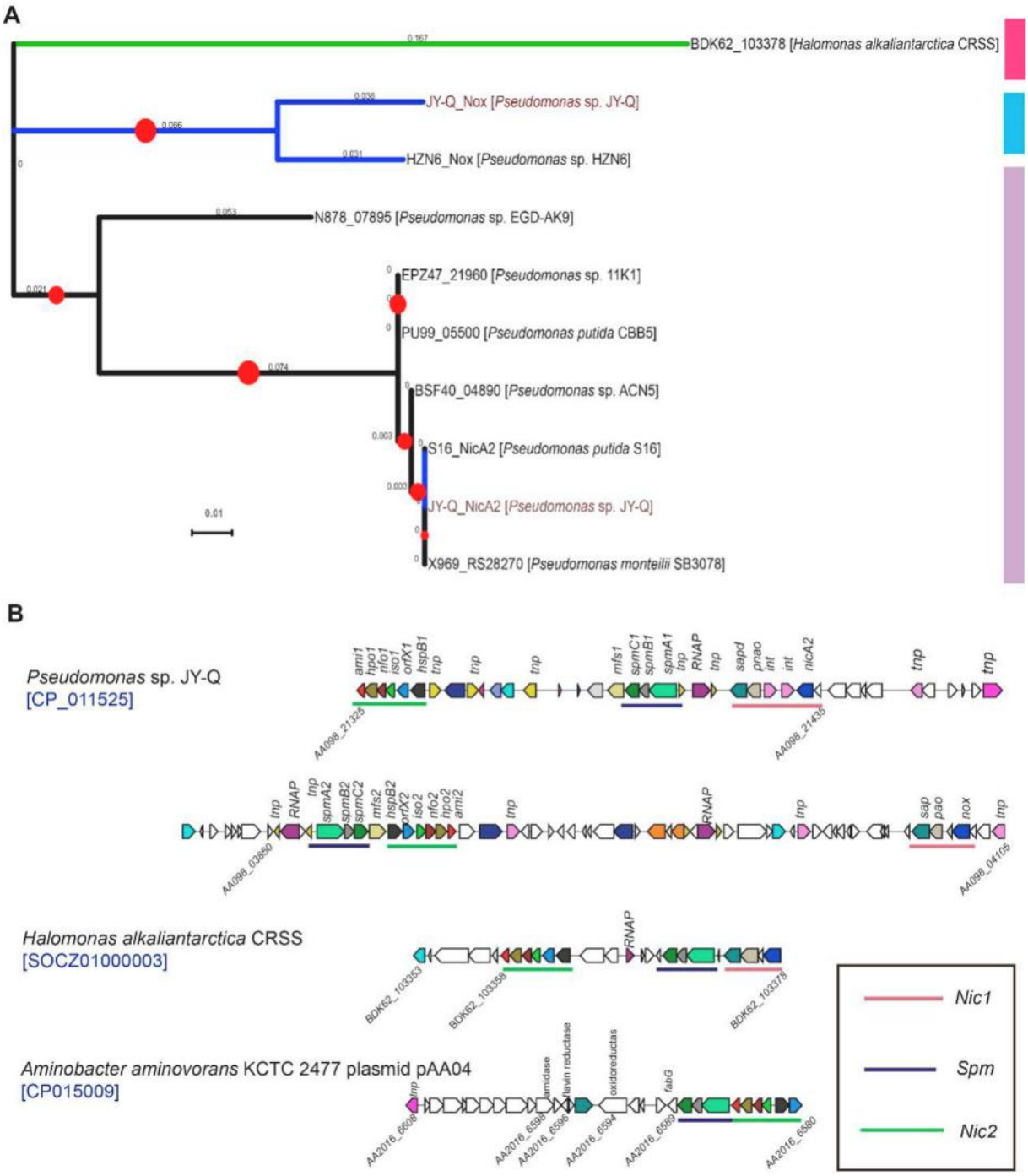


**Fig. 8. Phylogenetic relationships (A) and genomic contexts (B) of NicA2 and Nox**. Nic1: nicotine to 3-succinoylpyridine, Spm: 3-succinoylpyridine to 6-hydroxy-3-succinoylpyridine, Nic2: 6-hydroxy-3-succinoylpyridine to fumaric acid and succinic acid. Tnp: transposase, Int: Integrase, RNAP: RNA polymerase.

Nox were 0.346 mM and 0.225 mM, while the $k_{cat}/K_m$ values were 86.4 $mM^{-1}\ h^{-1}$ and 63.7 $mM^{-1}\ h^{-1}$, and the maximum velocity values were 532 $\mu M\ h^{-1}$ and 258 $\mu M\ h^{-1}$, respectively.

Based on the $k_{cat}/K_m$ and *K*m value, NicA2 exhibited higher efficiency but lower affinity for nicotine as substrate than Nox. Overall, NicA2 exhibits a better performance of nicotine transformation, but a little lower substrate affinity than Nox. Combined kinetic analysis and optimal condition examination suggests that the enzymatic features for NicA2 per unit are superior to those for Nox. However, Nox has a higher affinity for nicotine and biochemical stability than NicA2, although it is a less efficient dehydrogenase than NicA2.

### 3.6. Phylogeny relationship between these two homologous enzymes

Based on the bioinformatics analysis results, the stability/affinity difference between NicA2 and Nox may derive from their sequence variations. Moreover, in the whole pathway of nicotine metabolism, there are several couples of homologous genes: *nicA2* and *nox*, *sapd* and *sap*, *pao* and *pnao* [Fig. 1A and B]. As shown in Fig. 8A, the homologous genes, such as *nicA2* and *nox*, may result from different evolutionary process, based on the phylogeny assays. Phylogeny of NicA2 and Nox indicated that they could originate from different ancestors. The NicA2 ancestor could be *Halomonas* strains, suggesting that nicotine degrading genes might evolve from horizontal gene transfer (HGT) elements.

In Fig. 8B, the co-linear genomic comparison suggested potential genetic mobility in module Nic1 of strain JY-Q. Two integrase genes were localized between *nicA2* and *pnao*. The co-existence of three modules Nic1, Spm, and Nic2, were found in strain JY-Q and SB3078, while only Spm and Nic2 modules were found in *Aminobacter aminovorans* KCTC 2477 plasmid pAA04 and its genes of module Nic1 seemed to be 'deleted'. These findings suggest the possibility of Nic1 genomic transferability, which may contribute to the acquirement of co-existing homologous genes such as *nicA2* or *nox* in the same genome for Nic1.

## 4. Discussion

NicA2 and Nox are two homologous nicotine dehydrogenases that initiate the pyrrolidine degradation pathway [6,20]. The co-occurrence of NicA2 and Nox were identified in strain JY-Q, isolated from tobacco waste extract (TWE). Actually, an increasing number of findings on duplicated homologous genes for biodegradation were reported [30]. NicA2 and Nox exhibited additive effects on biodegradation of nicotine [15]. However, the homologous enzymes exhibited different contributions to biodegradation, because of their sequence and resultant structural differences.

In this study, the enzymatic characteristics of recombinant enzymes of homologous Nox and NicA2 were determined. The Nox highly expressed in wild type strain JY-Q exhibited lower *in vitro* catalytic activity as recombinant enzyme. While the NicA2 was under-expressed in wild type strain JY-Q exhibited higher *in vitro* catalytic activity as recombinant enzyme. In TWE containing high content nicotine, it might be reasonable to express more Nox (lower activity than NicA2) than NicA2 (higher activity than Nox), for less metabolic burden in JY-Q. In addition, Nox exhibited wide pH scale and higher temperature as optimal conditions for enzymatic reaction [Fig. 4]. The thermo-stability and acid-stability of Nox are both better than those of NicA2 [Fig. 5 and 6]. The reaction kinetics curve also showed that Nox had a lower Km and higher substrate affinity than NicA2 [Fig. 7]. These characteristics suggest that Nox has a greater role than NicA2 in TWE at low pH (4–5) and high temperature (above 40 °C). Nox was determined to possess superior enzymatic stability conferring a constant degradation efficacy for nicotine. In other words, it is necessary to enhance the affinity and suitability of NicA2 for further environmental remediation or public health through gene engineering [1,3,31,32].

The NicA2 structure has been reported [22]. Nox has 82% protein sequence identity with NicA2. The secondary structure of Nox protein is consistent with that of NicA2, comprising a FAD binding domain and a nicotine-binding domain. The FAD binding domain in Nox has a conserved structure like that in amine oxidases, of which amino acid residue W108, T248 and Q113 interact with the isoalloxazine ring, and adjacent amino acid residues W427 and N462 constitute an aromatic cage [2]. The nicotine-binding domain of Nox is similar to that of NicA2 with two subdomains. The activity difference of Nox and NicA2 may result from the variability of the 249th amino acid residue [NicA2:Glu (E249), Nox:Gln (Q245)] involved in nicotine binding [Fig. 1].

Generally, the flavin moiety in a flavoprotein, is the hydrogen acceptor in the oxidation process, which removes two hydrogen atoms from a substrate. We found that recombinant NicA2 and Nox exhibited very low activity in reaction mixture and their activities were improved significantly with additional $NAD^+$. This finding suggested that FAD covalently or tightly bind to NicA2 and Nox may not work well. Additional FAD also exhibited no effect on the activity of recombinant enzyme, the mechanism for this requires further study. We also observed a stoichiometry ratio of nicotine reduction and NADH generation of NicA2 and Nox close to the theoretical value (1:2) meaning that two hydrogen atoms all were transferred from nicotine to $NAD^+$ [Fig. 3]. However, the difference may result possibly from the slight oxidation of NADH or other factors and require further determination in future studies.

## Author contribution statement

**Jun Li**, Conceptualization, Resources, Data curation, Software, Formal analysis, Investigation, Methodology, Writing—original draft, Project administration, Writing-review and editing; **Mingjie Shen**, Data curation, Software, Formal analysis, Writing—original draft; **Zeyu Chen**, **Guoqing Chen**, Resources, Software, Formal analysis, Visualization, Methodology; **Fanda Pan, Yang Yang,** Investigation, Methodology; **Ming Shu**, **Yang Jiao**, Resources, Supervision, Investigation, Methodology; **Fuming Zhang, Robert J Linhardt**, Writing-review and editing; **Weihong Zhong**, Conceptualization, Resources, Supervision, Funding acquisition, Investigation, Methodology, Project administration, Writing-review and editing.

## Declaration of competing interest

All authors declare no conflict of interest in this work.

## Acknowledgement

This work was financially supported by grants from the National Natural Science Foundation of China (No. 31970104, 31670115 and 31800118), and the China Postdoctoral Science Foundation (2017M621965).

## References

[1] T. Thisted, Z. Biesova, C. Walmacq, E. Stone, M. Rodnick-Smith, S.S. Ahmed, S. K. Horrigan, B. Van Engelen, C. Reed, M.W. Kalnik, Optimization of a nicotine degrading enzyme for potential use in treatment of nicotine addiction, BMC Biotechnol. 19 (2019) 56.
[2] S. Xue, M. Kallupi, B. Zhou, L.C. Smith, P.O. Miranda, O. George, K.D. Janda, An enzymatic advance in nicotine cessation therapy, Chem. Commun. 54 (2018) 1686–1689.
[3] M. Kallupi, S. Xue, B. Zhou, K.D. Janda, O. George, An enzymatic approach reverses nicotine dependence, decreases compulsive-like intake, and prevents relapse, Sci. Adv. 4 (2018) eaat4751.
[4] H. Yu, R.P. Hausinger, H.Z. Tang, P. Xu, Mechanism of the 6-hydroxy-3-succinoyl-pyridine 3-monooxygenase flavoprotein from *Pseudomonas putida* S16, J. Biol. Chem. 289 (2014) 29158–29170.
[5] W. Wang, P. Xu, H. Tang, Sustainable production of valuable compound 3-succinoyl-pyridine by genetically engineering *Pseudomonas putida* using the tobacco waste, Sci. Rep. 5 (2015) 16411.
[6] H. Tang, L. Wang, W. Wang, H. Yu, K. Zhang, Y. Yao, P. Xu, Systematic unraveling of the unsolved pathway of nicotine degradation in *Pseudomonas*, PLoS Genet. 9 (2013), e1003923.
[7] H. Zhang, R. Zhao, C. Huang, J. Li, Y. Shao, J. Xu, M. Shu, W. Zhong, Selective and faster nicotine biodegradation by genetically modified *Pseudomonas* sp. JY-Q in the presence of glucose, Appl. Microbiol. Biotechnol. 103 (2019) 339–348.
[8] M. Mihasan, R. Brandsch, pAO1 of *Arthrobacter nicotinovorans* and the spread of catabolic traits by horizontal gene transfer in gram-positive soil bacteria, J. Mol. Evol. 77 (2013) 22–30.
[9] H. Yu, H. Tang, X. Zhu, Y. Li, P. Xu, Molecular mechanism of nicotine degradation by a newly isolated strain, *Ochrobactrum* sp. strain SJY1, Appl. Environ. Microbiol. 81 (2015) 272–281.
[10] L. Zhao, C. Zhu, Y. Gao, C. Wang, X. Li, M. Shu, Y. Shi, W. Zhong, Nicotine degradation enhancement by *Pseudomonas stutzeri* ZCJ during aging process of tobacco leaves, World J. Microbiol. Biotechnol. 28 (2012) 2077–2086.
[11] D. Pan, M. Sun, Y. Wang, P. Lv, X. Wu, Q.X. Li, H. Cao, R. Hua, Characterization of nicotine catabolism through a novel pyrrolidine pathway in *Pseudomonas* sp. S-1, J. Agric. Food Chem. 66 (2018) 7393–7401.
[12] G. Raman, K. Mohan, V. Manohar, N. Sakthivel, Biodegradation of nicotine by a novel nicotine-degrading bacterium, *Pseudomonas plecoglossicida* TND35 and its new biotransformation intermediates, Biodegradation 25 (2014) 95–107.
[13] P.F. Fitzpatrick, The enzymes of microbial nicotine metabolism, Beilstein J. Org. Chem. 14 (2018) 2295–2307.
[14] H. Hu, L. Wang, W. Wang, G. Wu, F. Tao, P. Xu, Z. Deng, H. Tang, Regulatory mechanism of nicotine degradation in *Pseudomonas putida*, mBio 10 (2019) e00602–19.
[15] J. Li, J. Wang, S. Li, F. Yi, J. Xu, M. Shu, M. Shen, Y. Jiao, F. Tao, C. Zhu, H. Zhang, S. Qian, W. Zhong, Co-occurrence of functional modules derived from nicotine-degrading gene clusters confers additive effects in *Pseudomonas* sp, JY-Q. Appl. Microbiol. Biotechnol. 103 (2019) 4499–4510.
[16] H. Tang, Y. Yao, L. Wang, H. Yu, Y. Ren, G. Wu, P. Xu, Genomic analysis of *Pseudomonas putida*: genes in a genome island are crucial for nicotine degradation, Sci. Rep. 2 (2012) 377.

[17] J. Qiu, Y. Ma, Y. Wen, L. Chen, L. Wu, W. Liu, Functional identification of two novel genes from *Pseudomonas* sp. strain HZN6 involved in the catabolism of nicotine, Appl. Environ. Microbiol. 78 (2012) 2154–2160.
[18] J. Li, S. Qian, L. Xiong, C. Zhu, M. Shu, J. Wang, Y. Jiao, H. He, F. Zhang, R. J. Linhardt, W. Zhong, Comparative genomics reveals specific genetic architectures in nicotine metabolism of *Pseudomonas* sp, JY-Q. Front. Microbiol. 8 (2017) 2085.
[19] H. Tang, L. Wang, X. Meng, L. Ma, S. Wang, X. He, G. Wu, P. Xu, Novel nicotine oxidoreductase-encoding gene involved in nicotine degradation by *Pseudomonas putida* strain S16, Appl. Environ. Microbiol. 75 (2009) 772–778.
[20] J. Qiu, Y. Ma, J. Zhang, Y. Wen, W. Liu, Cloning of a novel nicotine oxidase gene from *Pseudomonas* sp. strain HZN6 whose product nonenantioselectively degrades nicotine to pseudooxynicotine, Appl. Environ. Microbiol. 79 (2013) 2164–2171.
[21] S. Xue, J.E. Schlosburg, K.D. Janda, A new strategy for smoking cessation: characterization of a bacterial enzyme for the degradation of nicotine, J. Am. Chem. Soc. 137 (2015) 10136–10139.
[22] M.A. Tararina, K.D. Janda, K.N. Allen, Structural analysis provides mechanistic insight into nicotine oxidoreductase from *Pseudomonas putida*, Biochemistry 55 (2016) 6595–6598.
[23] M.A. Tararina, S. Xue, L.C. Smith, S.N. Muellers, P.O. Miranda, K.D. Janda, K. N. Allen, Crystallography coupled with kinetic analysis provides mechanistic underpinnings of a nicotine-degrading enzyme, Biochemistry 57 (2018) 3741–3751.
[24] W. Zhong, C. Zhu, M. Shu, K. Sun, L. Zhao, C. Wang, Z. Ye, J. Chen, Degradation of nicotine in tobacco waste extract by newly isolated *Pseudomonas* sp, ZUTSKD. Bioresour. Technol. 101 (2010) 6935–6941.
[25] R.C. Edgar, MUSCLE: multiple sequence alignment with high accuracy and high throughput, Nucleic Acids Res. 32 (2004) 1792–1797.
[26] M. Johnson, I. Zaretskaya, Y. Raytselis, Y. Merezhuk, S. McGinnis, T.L. Madden, NCBI BLAST: a better web interface, Nucleic Acids Res. 36 (2008) W5–W9.
[27] N.A. O'Leary, M.W. Wright, J.R. Brister, S. Ciufo, D. Haddad, R. McVeigh, B. Rajput, B. Robbertse, B. Smith-White, D. Ako-Adjei, A. Astashyn, A. Badretdin, Y. Bao, O. Blinkova, V. Brover, V. Chetvernin, J. Choi, E. Cox, O. Ermolaeva, C. M. Farrell, T. Goldfarb, T. Gupta, D. Haft, E. Hatcher, W. Hlavina, V.S. Joardar, V. K. Kodali, W. Li, D. Maglott, P. Masterson, K.M. McGarvey, M.R. Murphy, K. O'Neill, S. Pujar, S.H. Rangwala, D. Rausch, L.D. Riddick, C. Schoch, A. Shkeda, S.S. Storz, H. Sun, F. Thibaud-Nissen, I. Tolstoy, R.E. Tully, A.R. Vatsan, C. Wallin, D. Webb, W. Wu, M.J. Landrum, A. Kimchi, T. Tatusova, M. DiCuccio, P. Kitts, T. D. Murphy, K.D. Pruitt, Reference sequence (RefSeq) database at NCBI: current status, taxonomic expansion, and functional annotation, Nucleic Acids Res. 44 (2016) D733–D745.
[28] J. Li, C. Tai, Z. Deng, W. Zhong, Y. He, H.Y. Ou, VRprofile: gene-cluster-detection-based profiling of virulence and antibiotic resistance traits encoded within genome sequences of pathogenic bacteria, Briefings Bioinf. 19 (2018) 566–574.
[29] S. Kumar, G. Stecher, K. Tamura, MEGA7: molecular evolutionary genetics analysis version 7.0 for bigger datasets, Mol. Biol. Evol. 33 (2016) 1870–1874.
[30] T. Liu, J. Li, L. Qiu, F. Zhang, R.J. Linhardt, W. Zhong, Combined genomic and transcriptomic analysis of Dibutyl phthalate metabolic pathway in *Arthrobacter* sp, ZJUTW. Biotechnol. Bioeng. (2020), https://doi.org/10.1002/bit.27524.
[31] Z. Zhou, Y. Liu, G. Zanaroli, Z. Wang, P. Xu, H. Tang, Enhancing bioremediation potential of *Pseudomonas putida* by developing its acid stress tolerance with glutamate decarboxylase dependent system and global regulator of extreme radiation resistance, Front. Microbiol. 10 (2019) 2033.
[32] Z. Xia, L. Lei, H.Y. Zhang, H.L. Wei, Characterization of the ModABC molybdate transport system of *Pseudomonas putida* in nicotine degradation, Front. Microbiol. 9 (2018) 3030.